The current issue and full text archive of this journal is available at
**www.emeraldinsight.com/0332-1649.htm**



# Unconditionally stable improved meshless methods for electromagnetic time-domain modeling

Hooman Razmjoo
*Department of Electrical and Computer Engineering, Shiraz University, Shiraz, Iran, and*
Masoud Movahhedi
*Department of Electrical and Computer Engineering, Yazd University, Yazd, Iran*

**Abstract**

**Purpose** – In this paper, a modified meshless method, as one of the numerical techniques that has recently emerged in the area of computational electromagnetics, is extended to solving time-domain wave equation. The paper aims to discuss these issues.

**Design/methodology/approach** – In space domain, the fields at the collocation points are expanded into a series of new Shepard's functions which have been suggested recently and are treated with a meshless method procedure. For time discretization of the second-order time-derivative, two finite-difference schemes, i.e. backward difference and Newmark-$\beta$ techniques, are proposed.

**Findings** – Both schemes are implicit and always stable and have unconditional stability with different orders of accuracy and numerical dispersion. The unconditional stability of the proposed methods is analytically proven and numerically verified. Moreover, two numerical examples for electromagnetic field computation are also presented to investigate characteristics of the proposed methods.

**Originality/value** – The paper presents two unconditionally stable schemes for meshless methods in time-domain electromagnetic problems.

**Keywords** Electromagnetic CAD, Numerical analysis, Numerical methods

**Paper type** Research paper

## 1. Introduction

During the past decade, the application of meshfree or meshless methods to solve partial differential equations (PDEs) has been under a considerable attention in all engineering branches. In contradiction with finite element method (FEM), the meshless method can avoid the construction of tedious and difficult meshes and is very attractive in solving those problems that involve large deformations or problems with iterative adaptive mesh updating requirements. Meshless methods basically consist of the discretization of the problem domain and its boundary by a set of scattered points. Shape function or approximation function for each point is then constructed using its influence domain, which defines the relationship between a point and its neighbor points. The procedure for defining the shape function is still a central issue in meshless methods and it is one of the main differences in many implementations proposed in the literature.

COMPEL: The International Journal for Computation and Mathematics in Electrical and Electronic Engineering
Vol. 33 No. 1/2, 2014
pp. 463-482

0332-1649
DOI 10.1108/COMPEL-12-2012-0368

In Belytschko *et al.* (1996), the author introduced moving least square (MLS) method as a confident method to approach an approximation function. Babuska and Melenk (1997) proposed meshless and enhanced finite element procedures using hierarchical partition of unity (PU) interpolations. A newcomer meshless method based on natural element approximation has been used in Sukumar *et al.* (2001). The point interpolation method (PIM) is a meshfree interpolation technique that was used by Liu and Gu (2005) to construct shape functions using nodes distributed locally to formulate meshless weak-form methods. Two different types of PIM formulations are using the polynomial basis (Liu and Gu, 2001) and the radial basis functions (RBF), called radial point interpolation methods (RPIMs) (Wang and Liu, 2002). In Das and Lowther (2011) and Lima *et al.* (2012a, b), some recent developments of using RBFs in electromagnetic problems can be found. In Razmjoo *et al.* (2010a) a special class of partition of unity method (PUM) is used and its efficiency in electrostatic problems, Cartesian and polar coordinates has been verified. The distinguished advantage of this method is in non-uniform node distribution domain where the shape functions are constructed according to nodes density. Recently, a new method to resolve one of the biggest difficulties in meshless methods, i.e. shape function construction, has been engendered in Razmjoo *et al.* (2010a, b, 2011b, 2012). Based on the data fitting algorithm and PUM, a complete approach for constructing shape functions has been introduced and its performance in electromagnetic and electrostatic problems has been investigated. The proposed approximation functions show that they can reach acceptable accuracy in computational electromagnetics while their use saves a considerable computational time.

However, time domain implementation of the meshfree methods in computational electromagnetics has not still deliberated. Unfortunately, there are only a little literature which have employed space and time discretization schemes to discretize space and time in meshless method in electromagnetic problems. Some important cases: authors in Tanaka and Kunisada (2011) obtain vector potential in 2D time-domain problems. In their work, the problems are discretized using the RPIM for space and Newmark-$\beta$ method for time. In Razmjoo *et al.* (2011a), a new meshless approach is used to discretize space and a forward scheme of the finite-difference approximation is employed to expand time to solve wave equation. Chen *et al.* (2009) focused on space expansion by the method of weighted residuals (MWR) and time expansion by the finite-difference approximation of differential operators (Chen *et al.*, 2009). In Lai *et al.* (2008), a time domain meshless (RPIM) method (TDMM) is adopted for a 1D Maxwell's equations. In this paper, the authors employ a leap-frog scheme to discretize the problem in time and RPIM to discretize in space domains. In Yu and Chen (2009), 3D Maxwell's equations are solved in the same manner. In Yu and Chen (2010), Chen *et al.* (2011) and Mirzavand *et al.* (2012) two unconditionally stable meshless methods have been proposed with the implementation of the leapfrog alternating-direction-implicit (ADI) scheme and using weighted Laguerre polynomials in the 3D radial point interpolation meshless methods to solve the Maxwell equations. Moreover, in computational time-domain electromagnetics, we can point out to other meshless approaches such as smooth particle hydrodynamics (SPH) for electromagnetics (Ala *et al.*, 2006; Krohne *et al.*, 2008), the radial-point interpolation time-domain method in Kaufmann *et al.* (2008), the MLS reproducing kernel method (Viana and Mesquita, 1999) and the local Petrov-Galerkin (MLPG) approach (Soares, 2009).

As it was mentioned, different TDMMs in computational electromagnetics have been developed, recently (Tanaka and Kunisada, 2011; Razmjoo *et al.*, 2011a; Herault and Marechal, 1999; Fonseca *et al.*, 2008; Sukumar *et al.*, 2001; Chen *et al.*, 2009, 2011; Lai *et al.*, 2008; Yu and Chen, 2009, 2010; Kaufmann *et al.*, 2010). These schemes, like finite-element time-domain methods (Lee *et al.*, 1997), fall into two categories. One approach, which can be called second-order wave equation TDMM, is based on the discretization of the second-order vector wave equation, obtained by eliminating one of the field variables from Maxwell's equations. In this case, either the electric or the magnetic field is the only unknown (Tanaka and Kunisada, 2011; Razmjoo *et al.*, 2011a). Another approach which covers most of TDMMs is to construct meshless method for Maxwell's equations based on the discretization of two coupled first-order Maxwell curl equations. In this case, the electric field and the magnetic field are the simultaneous unknowns of the problem (Chen *et al.*, 2009, 2011; Lai *et al.*, 2008; Yu and Chen, 2009, 2010; Kaufmann *et al.*, 2010).

In Razmjoo *et al.* (2011a), an improved TDMM applied to the wave equation for analyzing transient electromagnetic fields was proposed and discussed. For this purpose, a recently proposed direct meshless method (Razmjoo *et al.*, 2011b), which is based on a new shape function, was adopted to discretize the space and a forward difference method for time discretization was used. In this paper, we focus on the time discretization of the wave equation. Two other finite difference schemes with different orders of accuracy and dispersion are used to discretize the time-derivative of the second-order wave equation. Employing these two schemes, i.e. Newmark-$\beta$ and backward difference methods for time discretization, are expected to yield unconditional stability, irrespective of time increment. The stability analysis of both schemes will be provided for meshless methods and various characteristics of them will be investigated.

The organization of this paper is as follows. Formulations of the proposed unconditionally stable direct meshless methods are first described. Then, numerical examples are presented to verify the effectiveness and efficiency of proposed method. Finally, the conclusions are made on the end.

## 2. Direct shape function

It is well-known that one of the biggest challenges in meshless methods is the shape function construction. Most of the conventional meshless methods need to compute the inversion of a matrix, which is usually an expensive process, to obtain the shape functions (Liu and Gu, 2005). In proposed procedure which has been introduced in Razmjoo *et al.* (2010a, b, 2011b), there is no need to do that; therefore, shape functions can be constructed faster. As mentioned, according to the data-fitting algorithm and PUM, a complete approach for constructing shape function of the meshless methods has been proposed, recently (Razmjoo *et al.*, 2010a, 2011b). A new weighting function is suggested so that shape function derivatives can be obtained easily in analytical forms (not numerical). Since, there is no mesh information, the essential boundary conditions can be imposed without any difficulty; also, interface conditions, as a result of physical discontinuities, would be imposed in a new and efficient manner.

In comparison with the most traditional schemes of meshless methods, it is simpler and faster in programming. However, its accuracy can be at the same level. This shape function would be used in this paper and for more details we refer readers to Razmjoo *et al.* (2011b).

Typically in a data fitting process, a fitting algorithm produces a function $F$ which is of the form $F(x) = \sum_i f_i N_i(x)$ where the values $f_i$s are known data (e.g. function values, derivatives, etc.). Functions $N_i$s are usually called shape functions. One class of fitting algorithms is based on the so-called "inverse distance weighted methods" whose ancestor is Shepard's (1968) method. In the basic Shepard method, scattered data $(x_i, f_i)$ is interpolated by a function as:

$$F(x) = \frac{\sum_i f_i \cdot w_i(x)}{\sum_i w_i(x)} \tag{1}$$

where the weights, i.e. $w_i(x)$s, are typically chosen as decaying functions of the distance $x$ from point $x_i$. The basic shape functions are thus as:

$$N_i(x) = \frac{w_i(x)}{\sum_i w_i(x)} \tag{2}$$

and the global approximation of $F$ takes the form:

$$F(x) = \sum_i f_i \cdot N_i(x) \tag{3}$$

Recently, we have proposed a new shape function with continuity and PU properties (Razmjoo *et al.*, 2011b), which are essential provisions of any shape function, directly. This function is as follows (for 1D):

$$N_i(x) = \frac{\exp(-\alpha|x - x_i|)}{\sum_j \exp(-\alpha|x - x_j|)} \tag{4}$$

In other words, the weights of the Shepard method in the proposed approach is as:

$$w_i(x) = w(x - x_i) = \exp(-\alpha|x - x_i|) \tag{5}$$

$\alpha$ is an independent positive coefficient which can change the overhang width of the shape function and its optimal setting increases the accuracy of the method. The proposed shape function in 2D and 3D can be achieved, similarly. Unlike PUM, there is no need to use more than one unknown per each node to achieve acceptable accuracy. Another advantage of the proposed shape function, unlike the shape function introduced in Razmjoo *et al.* (2010a), is that its derivatives can be obtained in analytical forms, simply, as have been given in Razmjoo *et al.* (2011a, b).

Since some of the shape functions used in the conventional meshless methods do not satisfy the Kronecker delta property (Belytschko *et al.*, 1996), the imposition of essential boundary conditions is another problem in these methods. A mixed formulation has been presented in Fonseca *et al.* (2010) which combines Shepard's shape functions for inner nodes to reduce the computational time and RPIM shape functions for boundary nodes to impose the essential boundary conditions. But, it is interesting to note that for the suggested direct shape function, smaller the overhang radius of the shape function using correct set of $\alpha$, closer to zero the value of the shape function in the other nodes. So, the boundary conditions will be enforced accurately without any problem (Herault and Marechal, 1999; Fonseca *et al.*, 2008).

Here, a 2D example is given to demonstrate the properties of the proposed shape function and its derivatives created using 25 nodes in a rectangular domain. Figure 1(a)-(d) shows the proposed shape function and its derivatives related to one of the middle nodes on an uniform $(5 \times 5)$ node distribution. Also, Figure 2 shows the shape functions of other two conventional meshless methods, that is, MLS approximation and thin plate spline radial point interpolation method (TPS-RPIM) (Sukumar *et al.*, 2001). As seen in Figures 1(a) and 2, the general form of the proposed shape function is similar to some of the other shape functions obtained by conventional meshless methods; except that the function can be obtained, directly, with a very low computational cost.

Simplicity of the proposed function leads to fast obtaining of all shape functions and decrease the simulation time of the meshless method based on the direct shape function. The time consumption for the shape function construction is shown in Figure 3 for two methods, the proposed method and RPIM approach. As seen, when the number of nodes, i.e. $M(=N^2)$ increases, the RPIM method processing time increases, extremely. This is due to the computation of a $(M \times M)$ matrix inversion for its shape functions construction. But, in the introduced method when the shape functions are constructed directly, there is no need to compute this matrix inversion. So, in the RPIM method, by increasing the number of nodes when the dimension of the resulted matrix is enlarged, the load of calculations would increase, extremely.

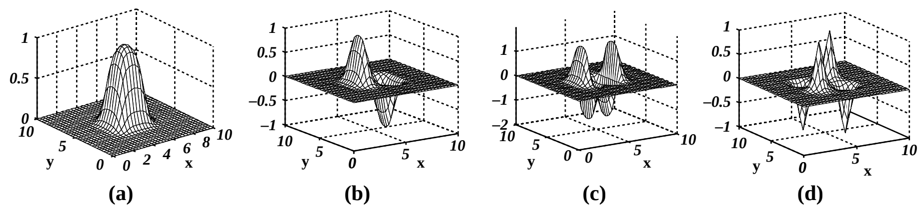


**Notes:** (a) Shape function $(N(x, y))$; (b) $(\partial N(x, y))/\partial x$; (c) $(\partial^2 N(x, y))/\partial x^2$; (d) $(\partial^2 N(x, y))/\partial x \partial y)$

**Figure 1.** Proposed shape function and its derivatives on a $(5 \times 5)$ uniform node distribution for one of the middle nodes

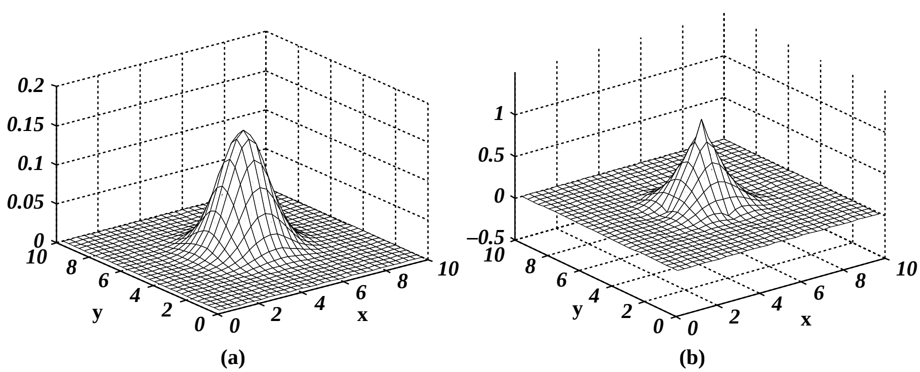


**Notes:** (a) MLS shape function; (b) TPS-RPIM shape function

**Figure 2.** Shape functions which are constructed by other two methods

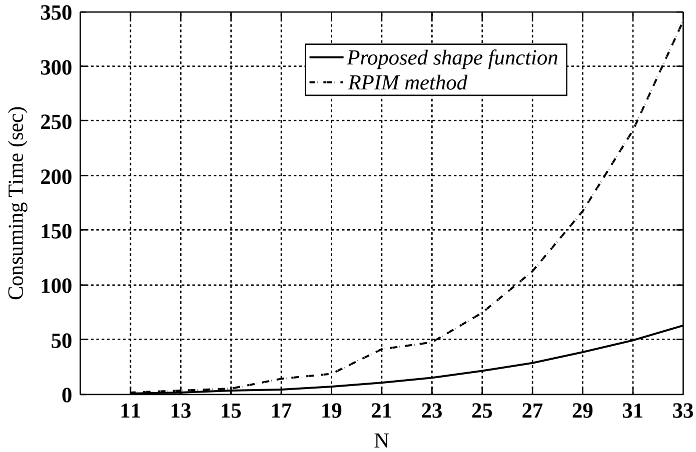


**Figure 3.**
Consuming time to construct the shape functions in proposed direct and RPIM-MQ methods for different number of nodes

## 3. Application to the wave equation

### *3.1 Governing equation*

Once the shape function and its derivatives are obtained, they can be used to meshless formulation of time-dependent vector wave equation.

Time-dependent electromagnetic fields radiated by an electric current density **J** are defined in a finite volume $\Omega$ bounded by surface $\partial\Omega$. The electric field must satisfy the time-dependent inhomogeneous wave equation, i.e.:

$$\nabla\times\frac{1}{\mu_r}\nabla\times\mathbf{E}+\frac{\varepsilon_r}{c_0^2}\frac{\partial^2\mathbf{E}}{\partial t^2}=-\mu_0\frac{\partial\mathbf{J}}{\partial t} \tag{6}$$

subject to the following boundary condition on $\partial\Omega(=\partial\Omega_e+\partial\Omega_h)$:

$$\hat{n}\times\mathbf{E}=0 \quad on \ \ \partial\Omega_e \tag{7}$$

$$\hat{n}\times(\nabla\times\mathbf{E})=0 \quad on \ \ \partial\Omega_h \tag{8}$$

where $c_0$ is the speed of light in free space, $\varepsilon_r$ and $\mu_r$ are the relative permittivity and permeability, respectively, and $\hat{n}$ represents the outward unit vector normal to $d\Omega$. The problem is simplified by defining $\partial\Omega$ to be a perfect electric conductor (PEC) surface on $\partial\Omega_e$ or perfect magnetic conductor (PMC) surface on $\partial\Omega_h$. Equation (6) can be simplified in three scalar equations like following scalar wave equation for $TM_z$ wave in a homogenous medium as follows (for 2D):

$$\frac{\partial}{\partial x}\left(\frac{1}{\mu_r}\frac{\partial E_z}{\partial x}\right)+\frac{\partial}{\partial y}\left(\frac{1}{\mu_r}\frac{\partial E_z}{\partial y}\right)+\frac{\varepsilon_r}{c_0^2}\frac{\partial^2 E_z}{\partial t^2}=-\mu_0\frac{\partial J_z}{\partial t} \tag{9}$$

Moreover, for other electric field components, the following scalar wave equations for 2D problems are considered:

$$\frac{\partial}{\partial x}\left(\frac{1}{\mu_r}\frac{\partial E_x}{\partial x}\right)+\frac{\partial}{\partial y}\left(\frac{1}{\mu_r}\frac{\partial E_x}{\partial y}\right)+\frac{\varepsilon_r}{c_0^2}\frac{\partial^2 E_x}{\partial t^2}=-\mu_0\frac{\partial J_x}{\partial t} \tag{10}$$

$$\frac{\partial}{\partial x}\left(\frac{1}{\mu_r}\frac{\partial E_y}{\partial x}\right)+\frac{\partial}{\partial y}\left(\frac{1}{\mu_r}\frac{\partial E_y}{\partial y}\right)+\frac{\varepsilon_r}{c_0^2}\frac{\partial^2 E_y}{\partial t^2}=-\mu_0\frac{\partial J_y}{\partial t} \tag{11}$$

To use the variational approach to formulate the meshless method, we first need to establish the required variational principle. For the problem above, it can be shown that its solution, for example for $E_z$, can be obtained by solving the equivalent variational problem defined by (Jin, 1993):

$$\delta F(E_z)=0 \tag{12}$$

where:

$$\begin{aligned}F(E_z)=&\frac{1}{2}\int\int_\Omega\left[\frac{1}{\mu_r}\left(\frac{\partial E_z}{\partial x}\right)^2+\frac{1}{\mu_r}\left(\frac{\partial E_z}{\partial y}\right)^2+\frac{\varepsilon_r}{c_0^2}\frac{\partial^2}{\partial t^2}E_z^2\right]d\Omega\\&+\int\int_\Omega\left[\mu_0\frac{\partial J_z}{\partial t}E_z\right]d\Omega\end{aligned} \tag{13}$$

It means that by minimizing equation (13) and enforcing essential boundary condition, $E_z$ can be obtained.

*3.2 Space-domain discretization*

Let us expand electric field components with the shape function introduced in Razmjoo *et al.* (2011b), for instance for $E_z$, as:

$$E_z(x,y,t)\simeq\sum_{i=1}^{M}N_i(x,y)\cdot e_{zi}(t) \tag{14}$$

where $N_i$s are the proposed shape functions, $e_{zi}(t)$ are the unknown coefficients which must be obtained and $M$ is the number of nodes. Substituting equation (14) into equation (13) and taking the derivative of $F$ with respect to $e_{zi}$, leads to the following second-order ordinary differential matrix form equation:

$$[K]\{e_z\}+\frac{1}{c_0^2}[K_\varepsilon]\frac{d^2}{dt^2}\{e_z\}=-\{f\} \tag{15}$$

where $[K]$ and $[K_\varepsilon]$ are time-independent matrices, $\{f\}$ is excitation vector, and:

$$K_{i,j}=\int\int_\Omega\left\{\frac{1}{\mu_r}\frac{\partial N_i}{\partial x}\frac{\partial N_j}{\partial x}+\frac{1}{\mu_r}\frac{\partial N_i}{\partial y}\frac{\partial N_j}{\partial y}\right\}d\Omega \tag{16}$$

$$K_{\varepsilon i,j}=\int\int_\Omega\{\varepsilon_r N_i\cdot N_j\}d\Omega \tag{17}$$

$$f_i = \int \int_{\Omega} \left\{ \mu_0 N_i \frac{\partial J_z}{\partial t} \right\} d\Omega \tag{18}$$

## 4. Time discretization and stability analysis

Here, two unconditionally stable meshless methods with implementation of the Newmark-$\beta$ and backward difference schemes for time discretization in solving wave equation by meshless method are proposed.

### *4.1 The Newmark-$\beta$ method*

Based on the Newmark-$\beta$ formulation for time discretization (Newmark, 1959; Zienkiewicz, 1977), equation (15) is approximated as:

$$\begin{aligned} &[K]\left(\beta\{e_z\}^{n+1} + (1-2\beta)\{e_z\}^n + \beta\{e_z\}^{n-1}\right) \\ &+ K_\varepsilon \frac{1}{(c_0\Delta t)^2}\left(\{e_z\}^{n+1} - 2\{e_z\}^n + \{e_z\}^{n-1}\right) \\ &= -(c_0\Delta t)^2(\beta\{f\}^{n+1} + (1-2\beta)\{f\}^n + \beta\{f\}^{n-1}) \end{aligned} \tag{19}$$

where, $\{e_z\}^n$ is the discrete-time representation of $\{e_z\}$, namely, $\{e_z\}^n = (n\Delta t)\{e_z\}$ and $\beta$ is a constant. This leads to an implicit update scheme as:

$$\{e_z\}^{n+1} = [A]^{-1}\left(2[B]\{e_z\}^n - [C]\{e_z\}^{n-1} + [D]\right) \tag{20}$$

where:

$$[A] = [K_\varepsilon] + \beta(c_0\Delta t)^2[K] \tag{21}$$

$$[B] = [K_\varepsilon] - 1/2(1-2\beta)(c_0\Delta t)^2[K] \tag{22}$$

$$[C] = -[K_\varepsilon] - \beta(c_0\Delta t)^2[K] \tag{23}$$

and:

$$[D] = -(c_0\Delta t)^2[\beta\{f\}^{n+1} + (1-2\beta)\{f\}^n + \beta\{f\}^{n-1}] \tag{24}$$

Stability analysis of equation (19) can be performed as follows. Equation (20) is expressed in reduced notation as the second-order difference equation:

$$\{e_z\}^{n+1} = 2[A]^{-1}[B]\{e_z\}^n - [A]^{-1}[C]\{e_z\}^{n-1} \tag{25}$$

where it is assumed $f = 0$. This can be rewritten as the following first-order equation:

$$\left\{ \begin{array}{c} \{e_z\}^{n+1} \\ \{e_z\}^n \end{array} \right\} = \begin{bmatrix} 2[A]^{-1}[B] & -[A]^{-1}[C] \\ 1[I] & [0] \end{bmatrix} \cdot \left\{ \begin{array}{c} \{e_z\}^n \\ \{e_z\}^{n-1} \end{array} \right\} \quad \{y\}^{n+1} = [M]\cdot\{y\}^n \tag{26}$$

Stability of the first-order equation requires $\rho([M]) < 1$, where $\rho([M])$ is the spectral radius of $[M]$. A thorough description of the stability analysis of the equation used here has been given in Gedney and Navsariwala (1999). It can be shown that the eigenvalues, $\xi$, of matrix $[M]$ are $\xi = \lambda_1 \pm \sqrt{\lambda_1^2 - \lambda_2}$, where:

$$\lambda_1 = \frac{1 - ((1-2\beta)/2) + \kappa(c_0\Delta t)^2}{1 + \kappa\beta(c_0\Delta t)^2 + (1/2)\eta_0 c_0 \Delta t(\sigma/\varepsilon_r)} \tag{27}$$

$$\lambda_2 = \frac{1 + \kappa\beta(c_0\Delta t)^2 - (1/2)\eta_0 c_0 \Delta t(\sigma/\varepsilon_r)}{1 + \kappa\beta(c_0\Delta t)^2 + (1/2)\eta_0 c_0 \Delta t(\sigma/\varepsilon_r)} \tag{28}$$

and:

$$\kappa = \frac{(\lambda_2 - 1) + (\lambda_2 + 1)\eta_0 c_0 \Delta t \sigma / 2\varepsilon_r}{\beta(c_0\Delta t)^2(1 - \lambda_2)} \tag{29}$$

where $\sigma$ is the medium conductivity that for simplicity has not been considered in the wave equation. Stability requires that $|\xi| < 1$, which is true if $|\lambda_2| < 1$, and $|\lambda_1| < (1 + \lambda_2)/2$. From above equation, it is seen that $|\lambda_2| < 1$ for all $\beta$. Finally, stability requires $|\lambda_1| < (1 + \lambda_2)/2$, which is true for all $\kappa \geq 0$ if $\beta > 1/4$. Since $\kappa_{max}$ is finite, then stability can be defined in the weak sense. Thus, choosing:

$$\beta \geq 1/4 \tag{30}$$

leads to unconditional stability of the second-order update expression (19).

It is interesting to note that the Newmark method is of second-order accuracy in time discretization and moreover, as stated, there is no limit on the size of $\Delta t$ for accuracy requirement.

### *4.2 Backward difference method*

If we apply the backward difference scheme to discretize the second time derivative of equation (15) at time step $(n+1)$, we obtain the backward difference representation of this equation as (Jin, 1993):

$$\left(\frac{1}{(\Delta t)^2}[K_\varepsilon] + c_0^2[K]\right)\{e_z\}^{n+1} = \frac{2}{(\Delta t)^2}[K_\varepsilon]\{e_z\}^n - \frac{1}{(\Delta t)^2}[K_\varepsilon]\{e_z\}^{n-1} - \{f\}^{n+1} \tag{31}$$

This scheme has first order of accuracy for time step. The stability analysis method employed here is based on the theory of discrete system analysis (Ziemer *et al.*, 1989; Jiao and Jin, 2002). Performing the $Z$ transform to equation (31), we obtain:

$$\left(\frac{1}{(\Delta t)^2}[K] + \frac{1}{c_0^2}[K_\varepsilon]\right)z^2\{\tilde{e}_z\} - \frac{2}{(\Delta t)^2}[K]z\{\tilde{e}_z\} + \frac{1}{(\Delta t)^2}[K]\{\tilde{e}_z\} = 0 \tag{32}$$

or:

$$-\frac{(z-1)^2}{z^2}\{\tilde{e}_z\} = \frac{(\Delta t)^2}{c_0^2}[K]^{-1}[K_\varepsilon]\{\tilde{e}_z\} \tag{33}$$

where $\{\tilde{e}_z\}$ denotes the $Z$-transform of $\{e_z\}^n$ and it is assumed $\{f\}^{n+2} = 0$. Clearly, $-(z-1)^2/z^2$ is the eigenvalue of the matrix $(\Delta t)^2/c_0^2[K]^{-1}[K_\varepsilon]$. Denoting this eigenvalue as $\lambda$, obviously $\lambda$ satisfies the following equation:

$$(z-1)^2 + \lambda z^2 = 0 \tag{34}$$

which is termed a characteristic equation here, since it carries the characteristic information of the stability criterion. The upper bound of $\lambda$, denoted as $\lambda_{max}$, indicates a relation between the maximum time step and the spatial discretization, which has to be satisfied to ensure stability. If $\lambda_{max}$ can reach the infinity, the scheme is unconditionally stable; because the time step is independent of spatial discretization and can be chosen arbitrarily; otherwise, the scheme is conditionally stable (Ziemer *et al.*, 1989). To determine $\lambda_{max}$, we can trace the roots of the characteristic equation in the complex plane. With $\lambda$ increasing to infinity, the roots of the characteristic equation change correspondingly. These roots are nothing but the poles of the linear system which can be seen clearly from equation (33). Hence, when the roots leave the unit circle in the complex plane (Ziemer *et al.*, 1989), the instability occurs. The value of $\lambda$ at this point yields the upper bound $\lambda_{max}$. To ensure stability, all eigenvalues of the matrix system should be smaller than $\lambda_{max}$, which indicates that the maximum eigenvalue $\left((\Delta t)^2/c_0^2\right)\rho([K]^{-1}[K_\varepsilon])$ should be smaller than $\lambda_{max}$.

The roots of equation (34) can be easily found as:

$$z = \frac{2 \pm \sqrt{-4\lambda}}{2(1+\lambda)} \tag{35}$$

whose magnitude is $1/\sqrt{1+\lambda}$. These roots never go beyond the unit circle in the complex plane because the eigenvalue is always non-negative. Hence, the stability of the backward difference scheme is unconditionally guaranteed.

It is important to note that although both Newmark-$\beta$ and backward difference schemes are unconditionally stable, they have different order of accuracy in time discretization and numerical dispersion which will be investigated in next section.

## 5. Numerical results

To demonstrate the validity of the proposed implementations of TDMM, at first, a 2D cavity with circular profile is chosen. The resonator corresponds to a cylindrical structure with infinite extension in its axial direction. The physical structure of the cylindrical cavity with radius 1 cm is shown in Figure 4. The vacuum cavity is enclosed by perfectly electric conducting wall. For comparative purposes, this cavity is simulated and the resonant frequency of its dominant mode, i.e. $TM_{01}$, is obtained by the meshless method with both implementations of time discretization methods, i.e. backward and Newmark-$\beta$ schemes. These two schemes are used in the meshless methods based on the proposed direct shape function and conventional RPIM method. A set of nodes, where the axial component of electric ($E$) field is stored, is distributed non-uniformly in the cavity volume. A sinusoidally modulated Gaussian pulse is used in this simulation as electric current source for problem excitation given by:

$$\mathbf{J} = A\cos(2\pi f_c t)\exp\left(-\left(\frac{t-t_0}{\tau}\right)\right)\hat{a}_z \tag{36}$$

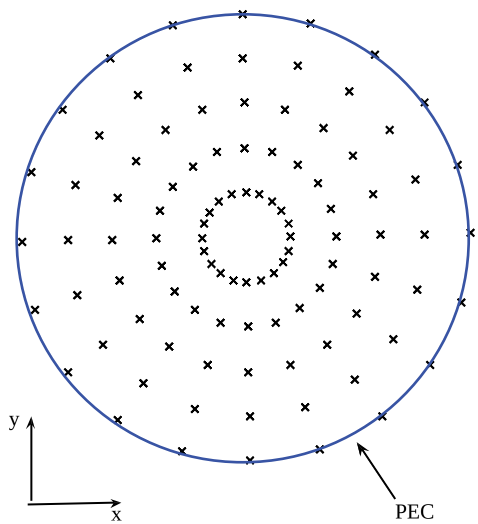


**Figure 4.** Depiction of the cylindrical cavity and its node arrangement

where $A = 10$, $f_c = 11\,\text{GHz}$, $\tau = 1/f_c$ and $t_0 = 4\tau$. This source is applied to a middle node of the cavity. Figure 5 shows this time function of the modulated Gaussian pulse excitation of the circular resonator. This example is a well-known problem with analytical solutions. Here, the *TM* case is considered with the electric field perpendicular to *z*-direction. By applying an analytical method for the structure analysis, the resonance frequencies of this problem can be obtained as:

$$f_{nm} = \frac{c}{2\pi}\left(\frac{\rho_{nm}}{r}\right) \tag{37}$$

where $\rho_{mn}$ is the $m$th root of Bessel's function of the first kind, i.e. $J_n$, $r$ is the radius of the cavity and $c$ is the light velocity. According to equation (37), exact resonant frequency of this structure for dominant mode of *TM* case is equal to 11.48 GHz.

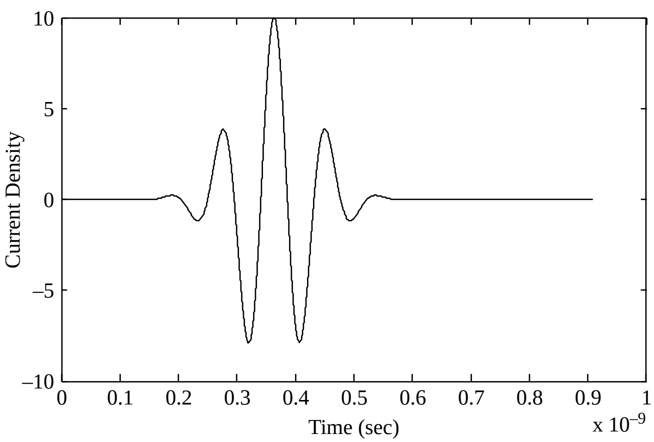


**Figure 5.** Time variations of the modulated Gaussian pulse excitation of the circular resonator

To solve 2D scalar wave equation in the cavity and obtain resonant frequency, for domain discretization, we use about 200 distinguished nodes (about ten nodes in the $\rho$-direction and 20 nodes in the $\phi$-direction) which are chosen in a radial strategy shown in Figure 4. $\alpha = 2/d_c$ is employed for the direct shape function where $d_c$ is the nodal spacing in each area (Razmjoo *et al.*, 2011b). Some of time discretization schemes which have been used in meshless method, are conditionally stable (Yu and Chen, 2009). In these approaches, the stability criterion for the meshless method is approximately (Yu and Chen, 2009):

$$\Delta t \leq \Delta t_{max} = d_{min}/c \tag{38}$$

where $d_{min}$ is the shortest nodal spacing between any two nodes in the computation domain and $c$ is the light velocity. Although such a condition guarantees the numerical stability, if the time step is very small, but it leads to a long time simulation that can make the meshless method impractical to use. As mentioned, two unconditionally stable methods for time discretization of meshless method were proposed. The first one was backward difference method which has an unconditional stability regardless of $\Delta t$. It means that the time steps can be chosen greater than criterion (38) to decrease the computational time. The time variation of the electric field recorded at an observation point, located at the center of the cavity, has been plotted in Figure 6(a), whereas its Fourier transform can be used to calculate resonant frequency of the cavity. In this simulation, $\Delta_t = 2.09 \times 10^{-12}$ s is used which is two times longer than $\Delta t_{max}$ calculated by equation (38). As this figure shows, the method is stable and the obtained resonant frequency, based on Figure 7(a), has acceptable accuracy. However, as seen in Figure 6(a), by choosing a great $\Delta t$, non-physical dispersion in the attenuation of the response amplitude, which is also evident in Razmjoo *et al.* (2011a), appear in simulation result. This matter is due to this fact that the phase velocity of numerical wave modes can differ from $c$ by an amount varying with the wavelength. This numerical dispersion is a factor in the time domain modeling that must be accounted for to understand its operation and its accuracy limits, especially for electrically large structures (Taflov and Hagness, 2000). Because of the use of a finite difference scheme for time descritization, numerical dispersion appears. An intuitive way to view this phenomenon is that the FDTD algorithm embeds the electromagnetic wave interaction structure of interest in a tenuous "numerical aether" having properties very close to vacuum, but not quite. This "aether" causes the propagation of numerical waves to accumulate delay or phase errors that can lead to non-physical results such as broadening and ringing of pulsed waveforms, imprecise cancellation of multiple scattered waves, anisotropy, and pseudo-refraction. Unfortunately, unlike some numerical methods such as FDTD, there is no way for meshless method to derive a relation for numerical dispersion, analytically. But it can be claimed, when the time step is smaller, numerical dispersion will decrease, reasonably. Moreover, the numerical result for the proposed direct meshless method based on the Newmark-$\beta$ scheme with $\beta = 0.5$ for the same time step, has been shown in Figure 6(b). This figure shows that by choosing the $\Delta t$ greater than criterion (38), the Newmark-$\beta$ method is also stable with lower dispersion error in comparison with the backward method. The Fourier transform of the time variant signals shown in Figure 6(a) and (b) are illustrated in Figure 7(a) and (b), respectively. As seen in these figures, resonant frequency is obtained accurately in both approaches. With the difference that the numerical dispersion causes the electric field obtained by backward

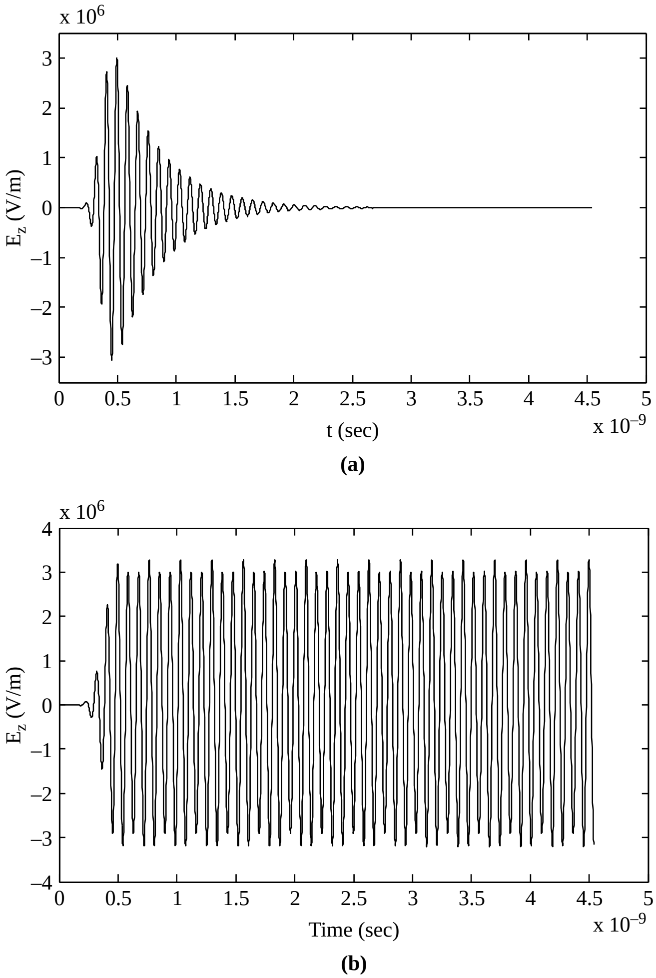


**Notes:** Time-domain electric fields at the observation point within the cavity recorded by proposed methods; (a) by backward scheme; (b) by Newmark-$\beta$ scheme

**Figure 6.**
Simulation results for the dominant mode in circular cavity

scheme to vanish. To have a quantitative comparison between the proposed meshless method based on the direct shape function and a conventional meshless method, i.e. RPIM, using backward and Newmark-$\beta$ time discritization schemes, the simulation results are given for the resonant frequency of the dominant mode of the cavity in Table I. As seen, the relative errors of the proposed unconditionally stable methods increase with the time step, while this increment is more for the backward method in contrast with the Newmark-$\beta$ scheme. These errors are completely due to the modeling accuracy of the numerical algorithm such as the numerical dispersion. The reduction in the number of

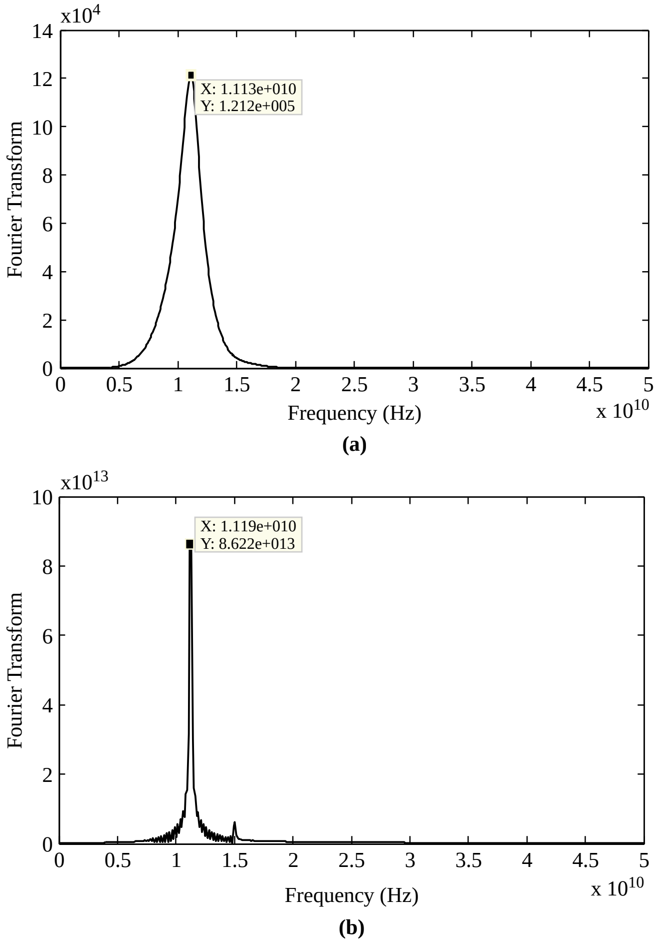


**Notes:** (a) Backward scheme; (b) Newmark-$\beta$ scheme

**Figure 7.**
Fourier transform of the electric fields recorded at the observation point of the circular cavity

**Table I.**
Comparison of the results of the Newmark-$\beta$ and backward schemes in TDMM for 2D circular cavity with different time steps

| $\Delta t$ | Proposed method (backward) Resonant frequency (GHz) | Proposed method (backward) Relative error (%) | Proposed method (Newmark-$\beta$) Resonant frequency (GHz) | Proposed method (Newmark-$\beta$) Relative error (%) | RPIM (backward) Resonant frequency (GHz) | RPIM (backward) Relative error (%) | RPIM (Newmark-$\beta$) Resonant frequency (GHz) | RPIM (Newmark-$\beta$) Relative error (%) |
|---|---|---|---|---|---|---|---|---|
| $Dt_{max}$ | 11.25 | 2.00 | 11.25 | 2.00 | 11.38 | 0.87 | 11.40 | 0.69 |
| $2Dt_{max}$ | 11.13 | 3.04 | 11.19 | 2.52 | 11.30 | 1.56 | 11.29 | 1.65 |
| $4Dt_{max}$ | 11.00 | 4.18 | 11.07 | 3.57 | 11.10 | 3.31 | 11.17 | 2.70 |
| $8Dt_{max}$ | 10.50 | 8.53 | 10.98 | 4.35 | 10.60 | 7.66 | 11.02 | 4.00 |

iterations and computational time occur by trading off techniques. Moreover, by increasing the time step, the proposed time discretization schemes applied to the proposed and RPIM meshless methods continue to produce stable results. It is important to note that, although, the RPIM results are little better than the proposed meshless method, but by more correct selection of the shape parameter, i.e. $\alpha$ (Razmjoo *et al.*, 2011b), the proposed meshless method can achieve the same level of accuracy, whereas the method can save a large part of the computational time.

To have a more difficult test on the proposed methods, a problem with complicated changes in its fields is investigated. It is related to a 2D rectangular cavity which is filled asymmetrically by a dielectric as shown in Figure 8. The dimensions of the cavity are $1.0\,\text{cm} \times 1.0\,\text{cm}$. This cavity is simulated and its dominant mode resonant frequency is obtained by the proposed meshless method with Newmark-$\beta$ scheme for time discretization. For comparative purposes, a similar cavity, but 3D with the same cross-section, is simulated by the CST Microwave Studio software as an accurate tool. It is well-known that because the field related to the dominant mode has no dependency on the third dimension, the dominant resonant frequency obtained by 3D simulation, can be achieved by similar 2D one. So, it can be an appropriate analogy to tell us about realistic accuracy of the proposed method.

CST Microwave Studio is a very powerful software in the electromagnetic computations. However, it employs "finite volume method", which is a different method from meshless methods, we can assure about its results accuracy and its results can be used for comparison purposes. In this comparison, only the accuracy of the proposed method has been tested. First, the dominant resonant frequency of the cavity will be obtained by the CST (eigenvalue solver) and then, it is compared with the obtained resonant frequency by proposed time domain method. Note that the eigenvalue solver does not use time descritization and so the dispersion error is not included.

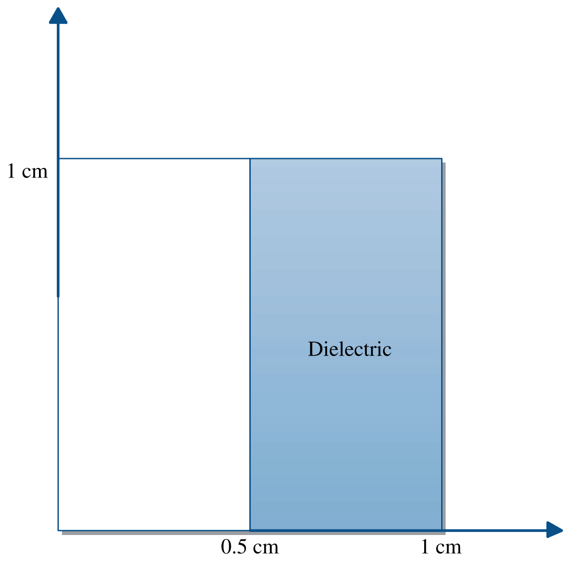


**Figure 8.**
Cross-section of a rectangular cavity filled by a dielectric rode

The computation domain was carried out using a uniform (10 × 10) node distribution. To construct direct shape functions, $\alpha_x = 2.5/d_x$ and $\alpha_y = 2.5/d_y$ are chosen where $d_x$ and $d_y$ are nodal spacing in *x*- and *y*-directions, respectively, (Razmjoo *et al.*, 2011b). Since, the structure resonant frequency is unknown in this case, a pulse excitation is used on a middle point of the domain. This excitation has a wide spectrum, so the true resonant frequency would be excited. On the cavity surfaces, which are assumed to be perfectly electric conducting walls, since the tangential components of the electric field is zero, a homogeneous Dirichlet boundary condition is imposed. Figure 9 shows the obtained resonant frequency by both methods for different values of $\varepsilon_r \cdot \Delta t = 4\Delta t_{max}$ is used here. As is expected, by increasing the dielectric constant, $\varepsilon_r$, the resonant frequency will be decreased. By setting $\varepsilon_r = 1$ it makes a simple cavity which $TM_{11}$ is its dominant mode. Figure 10(a) and (b) shows the time history for $E_y$ for the different nodes on the cavity plane, as obtained using the proposed method. The propagation of the electromagnetic fields related to the dominant mode is confirmed in these figures.

## 6. Conclusions

Two modified unconditionally stable meshless methods based on a new shape function in time domain for electromagnetic problems have been evaluated. The wave equation is discretized using a direct shape function for space domain. A method with acceptable accuracy along with low computation cost can be achieved using this shape function. For time discretization, the backward difference and Newmark-$\beta$ schemes are employed to simulate time domain problems by the weak-form meshless formulation. The stability analysis of both schemes has also been provided that shows the unconditional stability of such schemes. Although both schemes leads to unconditionally stable direct meshless methods, but numerical results show that the Newmark-$\beta$ scheme provides more accuracy and less numerical dispersion error.

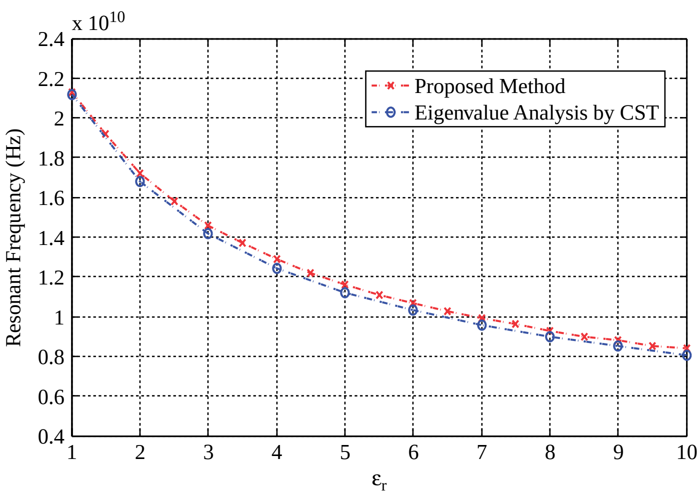


**Figure 9.**
Resonant frequency as a function of the rode dielectric constant computed by two methods

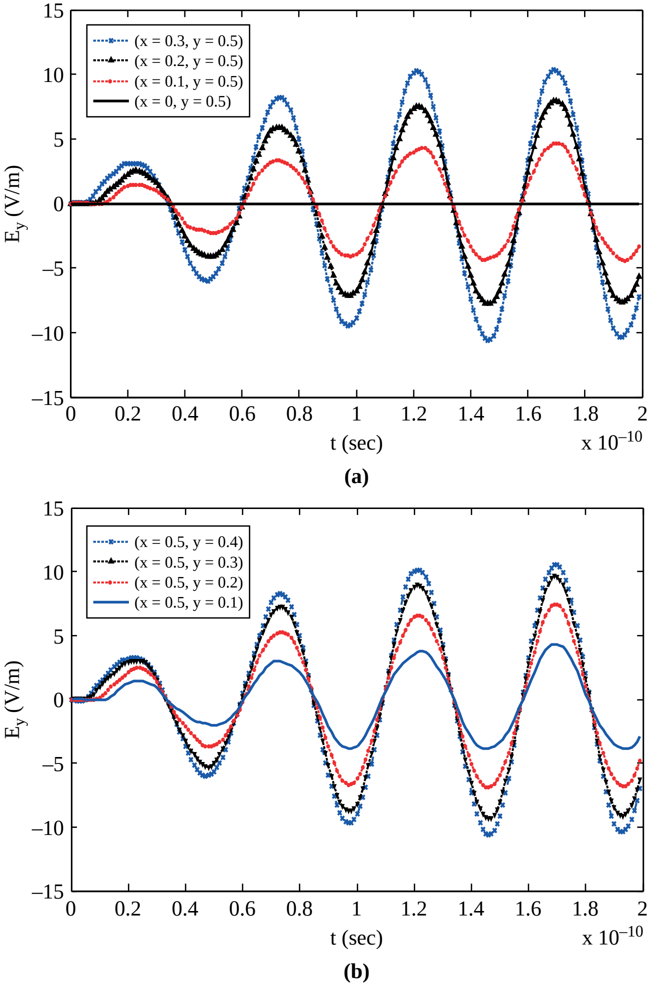


**Notes:** (a) On *y*-constant line; (b) on *x*-constant line

**Figure 10.**
Time history of $E_y$ in different nodes on cavity plane

## References

Ala, G., Francomano, E., Tortorici, A., Toscano, E. and Viola, F. (2006), "Smoothed particle electromagnetics: a mesh-free solver for transients", *J. Comput. Appl. Math.*, Vol. 191 No. 2, pp. 194-205.

Babuska, I. and Melenk, J.M. (1997), "The partition of unity method", *Int. J. Numer. Meth. Eng.*, Vol. 40, pp. 727-758.

Belytschko, T., Krongauz, Y., Organ, D., Fleming, M. and Krysl, P. (1996), "Meshless method: an overview and recent developments", *Comput. Meth. Appl. Mech. Eng.*, Vol. 139, pp. 3-47.

Chen, X., Chen, Z., Yu, Y. and Su, D. (2011), "An unconditionally stable radial point interpolation meshless method with Laguerre polynomials", *IEEE Trans. Antennas Propag.*, Vol. 59 No. 10, pp. 3756-3763.

Chen, Z., Yu, Y.Q. and Ney, M.M. (2009), "The time-domain method of weighted residuals (MWR): moving from grid-based methods to node-based meshless techniques", *Int. Conf. Electromagnetics in Advanced Applications, Italy, September*, pp. 200-203.

Das, R. and Lowther, D.A. (2011), "Magnetic field computation using compact support radial basis", *IEEE Trans. Magn.*, Vol. 47 No. 5, pp. 1362-1365.

Fonseca, A.R., Corra, B.C., Silva, E.J. and Mesquita, R.C. (2010), "Improving the mixed formulation for meshless local Petrov-Galerkin method", *IEEE Trans. Magn.*, Vol. 46 No. 8, pp. 2907-2910.

Fonseca, A.R., Viana, S.A., Silva, E.J. and Mesquita, R.C. (2008), "Imposing boundary conditions in the meshless local Petrov-Galerkin method", *IET Sci. Meas. Technol.*, Vol. 2 No. 6, pp. 387-394.

Gedney, S.D. and Navsariwala, U. (1999), "An unconditionally stable finite element time-domain solution of the vector wave equation", *IEEE Microw. Guided Wave Lett.*, Vol. 35 No. 3, pp. 1450-1453.

Herault, C. and Marechal, Y. (1999), "Boundary and interface conditions in meshless methods", *IEEE Trans. Magn.*, Vol. 35 No. 3, pp. 1450-1453.

Jiao, D. and Jin, J.M. (2002), "A general approach for the stability analysis of the time-domain finite-element method for electromagnetic simulations", *IEEE Trans. Microw. Theory Tech.*, Vol. 50 No. 11, pp. 1624-1632.

Jin, J.M. (1993), *The Finite Element Method in Electromagnetics*, Wiley, New York, NY.

Kaufmann, T., Fumeaux, C. and Vahldieck, R. (2008), "The meshless radial point interpolation method for time-domain electromagnetics", *IEEE MTT-S Int. Microw. Symp. Dig., Atlanta, GA, June*, pp. 61-65.

Kaufmann, T., Engstorm, C., Fumeaux, C. and Vahldieck, R. (2010), "Eigenvalue analysis and longtime stability of resonant structures for the meshless radial point interpolation method in time domain", *IEEE Trans. Microw. Theory Tech.*, Vol. 58 No. 12, pp. 3399-3408.

Krohne, K., Park, G.H. and Ping, L.E. (2008), "A two-dimensional smoothed particle time-domain method", *Asia-Pacific Microw. Conf. Proc., Hong Kong, December*, pp. 1-4.

Lai, S.J., Wang, B.Z. and Duan, Y. (2008), "Meshless radial basis function method for transient electromagnetic computations", *IEEE Trans. Magn.*, Vol. 44 No. 10, pp. 2288-2295.

Lee, J.F., Lee, R. and Cangellaris, A.C. (1997), "Time-domain finite element methods", *IEEE Trans. Antennas Propagat.*, Vol. 45 No. 3, pp. 430-442.

Lima, N.Z., Fonseca, A.R. and Mesquita, R.C. (2012a), "Application of local point interpolation method to electromagnetic problems with material discontinuities using a new visibility criterion", *IEEE Trans. Magn.*, Vol. 48 No. 2, pp. 615-618.

Lima, N.Z., Mesquita, R.C., Facco, W.G., Moura, A.S. and Silva, E.J. (2012b), "The nonconforming point interpolation method applied to electromagnetic problems", *IEEE Trans. Magn.*, Vol. 48 No. 2, pp. 619-622.

Liu, G.R. and Gu, Y.T. (2001), "A point interpolation method for two-dimensional solids", *Int. J. Numer. Meth. Eng.*, Vol. 50, pp. 937-951.

Liu, G.R. and Gu, Y.T. (2005), *An Introduction to Meshfree Methods and Their Programming*, Springer, Berlin.

Mirzavand, R., Abdipour, A., Moradi, G. and Movahhedi, M. (2012), "Unconditionally stable MFLTD method for the full wave electromagnetic simulation", *IEEE Trans. Antennas Propag.*, Vol. 60 No. 5, pp. 2583-2586.

Newmark, N.M. (1959), "A method of computation for structural dynamics", *J. Engineering Mechanics Division. ASCE*, Vol. 85, pp. 67-94.

Razmjoo, H., Movahhedi, M. and Hakimi, A. (2010a), "An efficient meshless method based on a new shape function", *Int. J. Numer. Modelling: Electronic Networks, Devices and Fields*, Vol. 23 No. 6, pp. 503-521.

Razmjoo, H., Movahhedi, M. and Hakimi, A. (2010b), "Improved meshless method using direct shape function for computational electromagnetics", *Asia-Pacific Microw. Conf. Proc., Japan, December*, pp. 2157-2160.

Razmjoo, H., Movahhedi, M. and Hakimi, A. (2011a), "Electromagnetic time domain modeling using an improved meshless method", *IEEE MTT-S Int. Microw. Symp. Dig., Baltimore, June*, pp. 1-4.

Razmjoo, H., Movahhedi, M. and Hakimi, A. (2011b), "Modification on a fast meshless method for electromagnetic field computations", *IET Sci. Meas. Technol.*, Vol. 5 No. 5, pp. 175-182.

Razmjoo, H., Movahhedi, M. and Hakimi, A. (2012), "An improved truly meshless method based on a new shape function and nodal integration", *Int. J. Numer. Modelling: Electronic Networks, Devices and Fields*, Vol. 25 Nos 5/6, pp. 441-453.

Shepard, D. (1968), "A two dimensional interpolation function for irregularly spaced data", *23rd Nat. Conf. ACM*, pp. 517-523.

Soares, D. Jr (2009), "Numerical modelling of electromagnetic wave propagation by meshless local Petrov-Galerkin formulations", *Computer Modeling in Engineering and Sciences*, Vol. 50 No. 2, pp. 97-114.

Sukumar, N., Moran, B., Semenov, A. and Belikov, V. (2001), "Natural neighbor Galerkin methods", *Int. J. Numer. Meth. Eng.*, Vol. 50, pp. 1-27.

Taflov, A. and Hagness, S.C. (2000), *Computational Electromagnetics: The Finite-Difference Time-Domain Method*, Artech House, London.

Tanaka, Y. and Kunisada, E. (2011), "Study on meshless method using RPIM for transient electromagnetic field", *IEEE Trans. Magn.*, Vol. 47 No. 5, pp. 1178-1181.

Viana, S.A. and Mesquita, R.C. (1999), "Moving least square reproducing kernel method for electromagnetic field computation", *IEEE Trans. Magn.*, Vol. 35 No. 3, pp. 1372-1375.

Wang, J.G. and Liu, G.R. (2002), "A point interpolation meshless method based on radial basis functions", *Int. J. Numer. Meth. Eng.*, Vol. 54 No. 11, pp. 1623-1648.

Yu, Y. and Chen, Z. (2009), "A 3D radial point interpolation method for meshless time-domain modeling", *IEEE Trans. Microw. Theory Tech.*, Vol. 57 No. 8, pp. 2015-2020.

Yu, Y. and Chen, Z. (2010), "Towards the development of an unconditionally stable time-domain meshless method", *IEEE Trans. Microw. Theory Tech.*, Vol. 58 No. 3, pp. 578-586.

Ziemer, R.E., Tranter, W.H. and Fannin, D.R. (1989), *Signals and Systems: Continuous and Discrete*, Macmillan, New York, NY.

Zienkiewicz, O.C. (1977), "A new look at the Newmark, Houboult and other time stepping formulas: a weighted residual approach", *Earthquake Engineering and Structural Dynamics*, Vol. 5, pp. 413-418.

## About the authors

Hooman Razmjoo was born in Shiraz, Iran, on September 6, 1986. He received the BSc degree in electrical engineering from Shahid Bahonar University of Kerman, Kerman, Iran, in 2008. He is currently working toward the MSc degree in the Department of Electrical Engineering at the same university. His research interests include the computational electromagnetics and high-frequency circuit simulation.

Masoud Movahhedi was born in Yazd, Iran, in 1976. He received the BSc degree from Sharif University of Technology, Tehran, Iran, in 1998, the MSc and PhD degrees from Amirkabir

University of Technology (Tehran Polytechnic), Tehran, Iran, in 2000 and 2007, all in electrical engineering. From December 2005 to September 2006, he was with the Institute for Microelectronics, Technische Universitat Wien, Austria, as a visiting student. He was with the Electrical Engineering Department, Shahid Bahonar University of Kerman, Kerman, Iran, and is currently an Assistant Professor with the Electrical And Computer Engineering Department, Yazd University, Yazd, Iran. His research interests are in the areas of computer-aided design of microwave integrated circuits, computational electromagnetic, semiconductor high-frequency RF modeling, and interconnect simulations. Dr Movahhedi was the recipient of the GAAS-05 Fellowship sponsored by the GAAS Association to young graduate researchers for his paper presented at GAAS2005. He was also the recipient of the Electrical Engineering Department Outstanding Student Award in 2005 and 2006. Masoud Movahhedi is the corresponding author and can be contacted at: movahhedi@ieee.org